



# Mapping size-specific phytoplankton primary production on a global scale

ROBERT J. W. BREWIN<sup>1</sup>, SAMANTHA J. LAVENDER<sup>2</sup> and NICK J. HARDMAN-MOUNTFORD<sup>3</sup>

<sup>1</sup>School of Marine Science and Engineering, University of Plymouth. Drake Circus, Plymouth, PL4 8AA, UK; [robert.brewin@plymouth.ac.uk](mailto:robert.brewin@plymouth.ac.uk).

<sup>2</sup>ARGANS Ltd, Unit 3, Drake Building, Tamar Science Park, Derriford, Plymouth, PL6 8BY, UK.

<sup>3</sup>Plymouth Marine Laboratory, Prospect Place, The Hoe, Plymouth, PL1 3DH, UK.

## Abstract

Since the formation of satellite-borne visible spectral radiometry (ocean colour), oceanographers have developed techniques to map phytoplankton biomass on a global scale, with a major application being to model primary production and the ocean carbon cycle in the context of climate change. However, we now recognise that marine carbon cycling links specifically to the activity of particular phytoplankton functional groups. From the perspective of primary production and the global carbon cycle, cell size is thought to be sufficient for defining these functional groups. This has led to a variety of bio-optical methods that use satellite data to differentiate between phytoplankton size classes. Here we combine an established phytoplankton size class algorithm which is integrated into an available-light primary production model in order to partition and map primary production estimates from microplankton ( $>20\mu\text{m}$ ) and combined nano-picoplankton ( $<20\mu\text{m}$ ) on a global scale for the year 2005. We estimate global primary production in 2005 to be  $51.20 \pm 0.29 \text{ Gt C y}^{-1}$  of which, combined nano-picoplankton contributes to  $48.58 \pm 0.34 \text{ Gt C y}^{-1}$  (94.8%) and microplankton  $2.62 \pm 0.07 \text{ Gt C y}^{-1}$  (5.2%). This approach can supply data for large-scale maps of size-specific primary production and an example of May and November 2005 is shown.

(Received 19<sup>th</sup> October 2009; Revised 18<sup>th</sup> December 2009; Accepted 21<sup>st</sup> December 2009)



## 1. Introduction

Since the establishment of the industrial revolution at the beginning of the 19th Century, there has been a vast increase in anthropogenic emissions of carbon dioxide (CO<sub>2</sub>) from the burning of fossil fuels or deforestation. CO<sub>2</sub> released into the atmosphere may have three possible fates: it may be absorbed by the terrestrial ecosystem, absorbed by the ocean, or it may continue to reside in the atmosphere (Nair et al., 2008). The ocean has been found to contribute to 45% of global primary production of CO<sub>2</sub> (Falkowski et al., 2004; Longhurst et al., 1995; Field et al., 1998) and be responsible for absorbing 26% of anthropogenic CO<sub>2</sub> released into the atmosphere (House et al., 2002).

In light of increasing concern about the accelerating greenhouse effect, oceanographers are required to develop techniques to monitor synoptically the health of our oceans. Currently, the only practical way of synoptically mapping phytoplankton abundance is through satellite remote sensing. Traditionally, bio-optical models have been used that categorise phytoplankton under a single group using specific biomarkers (e.g. chlorophyll-a). However, marine carbon cycling is specifically linked to the activity of particular phytoplankton functional groups (Le Quéré et al., 2005).

From the perspective of primary production and the global carbon cycle, cell size, referred to here as phytoplankton size class (PSC) is thought to be sufficient for defining the functional groups (Sieburth et al., 1978; Aiken et al., 2009; Chisholm, 1992). This has led to a variety of satellite bio-optical models designed to distinguish between PSCs (Hirata et al., 2008; Uitz et al., 2006; Ciotti and Bricaud, 2006; Devred et al., 2006).

A number of algorithms have also been developed that estimate global distributions of primary production from satellite derived chlorophyll-a data (Behrenfeld and Falkowski, 1997a;b; Morel, 1991; Platt and Sathyendranath, 1988; Platt et al., 1980; Sathyendranath et al., 1995). Such algorithms can be categorised into either available-light models, absorbed-light models, biomass-independent models, growth models, or spectral models (Sathyendranath and Platt, 2007).

The objective of this paper is to develop a size-specific primary production model by integrating the phytoplankton size class model of Devred et al. (2006), developed from theory proposed in Sathyendranath et al. (2001), into an available-light primary production model (e.g. Platt et al., 1980). An estimate of the biomass and photophysiological parameters needed to calculate the primary production of two respective phytoplankton size classes (microplankton >20µm and combined nano- and picoplankton <20µm) are thus inferred from the knowledge of chlorophyll-a, light intensity, and diffuse attenuation. Size-specific primary production is then calculated for each month in 2005 and mapped for two contrasting months in 2005 (May and November) using the proposed primary production model and satellite data.

## 2. Data

For the present study, the method of Vidussi et al. (2001), extended by Uitz et al. (2006), which uses seven diagnostic pigments to obtain the fraction of combined nano- and picoplankton ( $F_1$ ) and microplankton ( $F_2$ ) from *in situ* pigment data, was applied to a large High Performance Liquid Chromatography (HPLC) pigment dataset (3255 measurements) from the Atlantic Meridional Transect (AMT) database and the NASA NOMAD database (Werdell and Bailey, 2005). The pigment data was strictly quality controlled according to Aiken et al. (2009) reducing the number of measurements to 2761. These fractions were then applied to the actual *in situ* chlorophyll-a concentration (here after denoted [chl]) in order to calculate size-specific [chl] of combined nano- and picoplankton [ $chl_1$ ] and microplankton [ $chl_2$ ] from the *in situ* pigment data.

Behrenfeld and Falkowski (1997b) assembled a dataset of primary production measured by the  $^{14}\text{C}$  method (Steeman-Nielsen, 1952). This dataset provided coupled data on position, date, daily-integrated photosynthetically active radiation (PAR) above the sea-surface, euphotic depth (depth at which PAR is reduced to 1% of its surface value), the optical depth ( $\tau$ ), primary production, and [chl]. The dataset was extracted from the Website of Rutgers University (<http://marine.rutgers.edu/opp/>) and provided 15,013 individual measurements. A map of the *in situ* data used for this study is given in Figure 1.

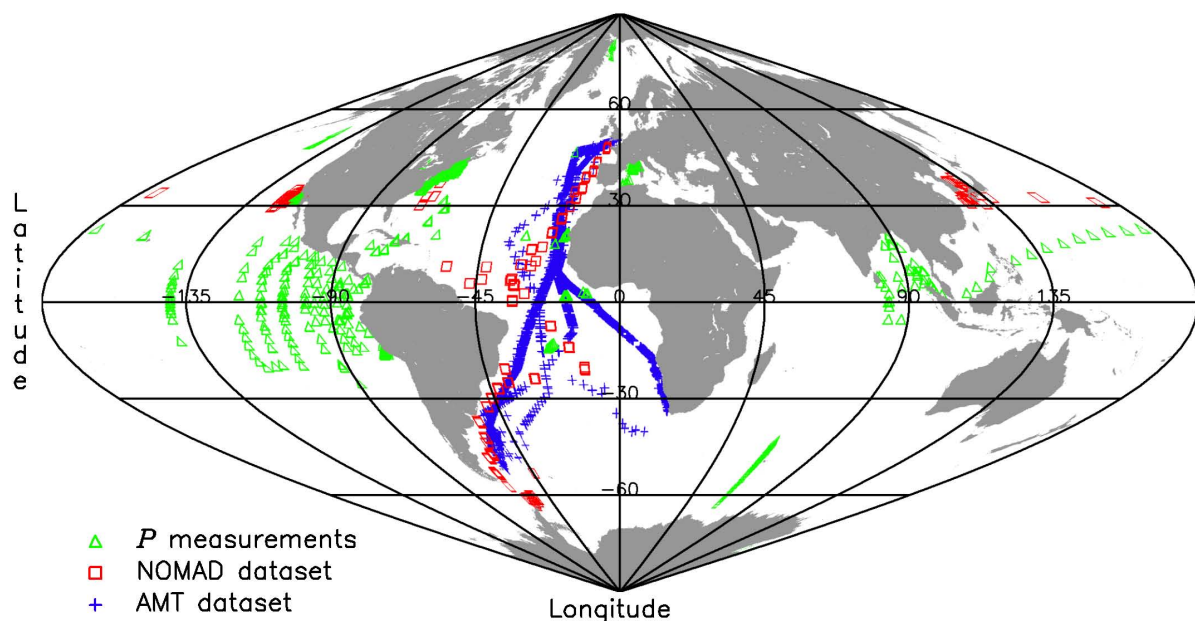


Figure 1. Locations of the *in situ* data used in this study

### 3. Methodology

Here, as in the Devred et al. (2006) model, following the theory of Sathyendranath et al. (2001), [chl] can be expressed as the sum of [chl<sub>1</sub>] and [chl<sub>2</sub>], such that [chl] = [chl<sub>1</sub>] + [chl<sub>2</sub>]. We fitted the Devred et al. (2006) model (Devred et al., 2006, Equation 2) to [chl<sub>1</sub>] and [chl] from the *in situ* pigment data in order to derive the parameters of C<sub>1</sub><sup>m</sup> and S. The model was fitted to pigment data using a standard nonlinear least squares method (Levenberg-Marquardt, Press et al. (1992), IDL Routine MPFITFUN). Logarithmic transformation was applied to both [chl<sub>1</sub>] and [chl] in order to down-weight the influence of very large data points. Parameter values for C<sub>1</sub><sup>m</sup> and S are given in Table 1, and Figure 2 shows the model plotted against the observations which indicates a good fit as highlighted by the low mean errors (ME). Having derived these parameters [chl<sub>1</sub>], [chl<sub>2</sub>], F<sub>1</sub> and F<sub>2</sub> can be directly estimated from the total chlorophyll-a concentration [chl] (Equations 2 and 12, Devred et al., 2006).

Population	C <sub>1</sub> <sup>m</sup>	S	P <sub>ms</sub> <sup>b</sup> (mg C (mg [chl] <sup>-1</sup> h <sup>-1</sup>	β <sub>p</sub>	< α <sub>s</sub> <sup>b</sup> > (mg C (mg [chl] <sup>-1</sup> h <sup>-1</sup> ) [μ mol quanta m <sup>-2</sup> s <sup>-1</sup> ] <sup>-1</sup> )	β <sub>α</sub>
Combined nano-picoplankton (Subscript 1)	1.180	0.780	6.107	-0.063	0.230	-0.463
Microplankton (Subscript 2)	-	-	1.570	0.073	0.015	0.371

Table 1. Parameters derived for the size-specific P model.

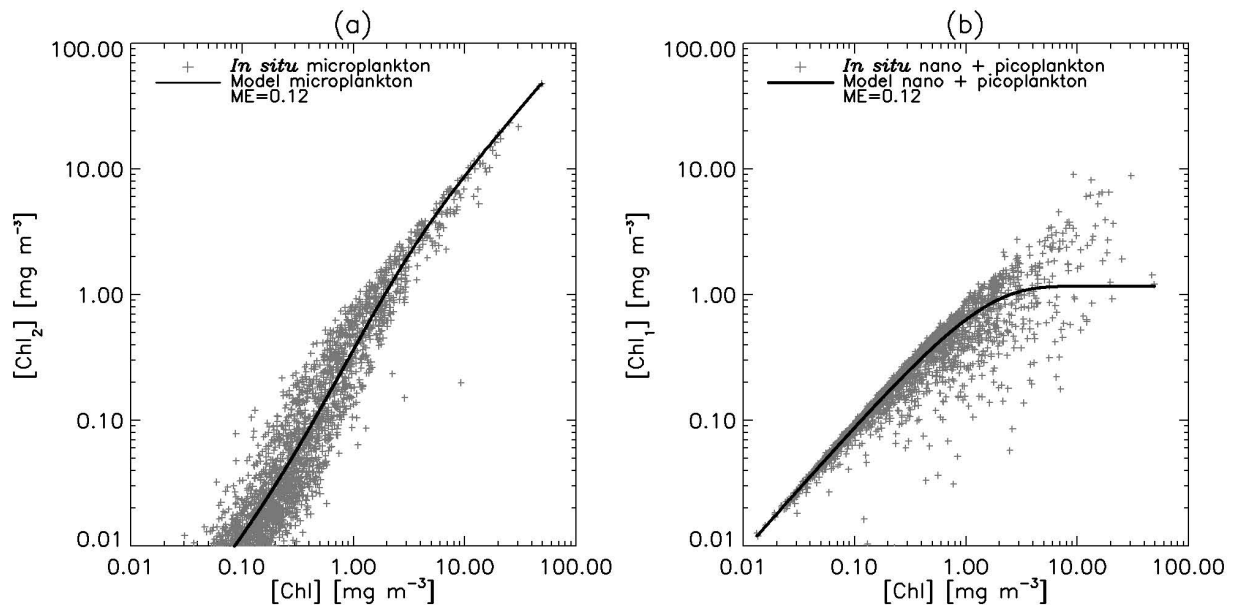


Figure 2. Devred et al. (2006) model fitted to *in situ* data from AMT and NOMAD database (a) [chl<sub>2</sub>] plotted against [chl] and (b) [chl<sub>1</sub>] plotted against [chl].

Primary production ( $P$ ) can be calculated as a function of the chlorophyll-normalised primary production ( $P^b$ ) and [chl], such that  $P = P^b[\text{chl}]$ . Available-light or photosynthe-

sis-irradiance models of primary production that are formulated as functions of available light make use of equations such as the following (Platt et al., 1980):

$$P^b = P_m^b \left[ 1 - \exp \left( - \frac{\langle \alpha^b \rangle}{P_m^b} \text{PAR} \right) \right] \quad (1)$$

where, the chlorophyll-normalised primary production ( $P^b$ ) is calculated using  $\langle \alpha^b \rangle$ , the initial slope measured for a flat incident spectral light field covering the entire photosynthetically-active wavelength domain, and  $P_m^b$ , the assimilation number of the light-saturation curve, both normalised by the chlorophyll-a concentration. Assuming  $P^b$  comprises a sum of the combined nano-picoplankton population and the microplankton population, one can assume  $P^b = P_1^b F_1 + P_2^b F_2$ .

Uitz et al. (2008) showed that the size-specific photophysiological parameters ( $P_m^b$ ) and  $\langle \alpha^b \rangle$  are significantly correlated with the optical depth ( $\tau$ ) and that the relationship can be described by an exponential equation, where,  $P_{ms}^b$  and  $\langle \alpha_s^b \rangle$  represent  $P_m^b$  and  $\langle \alpha^b \rangle$  at the surface, where  $\tau = 0$ , and  $\beta_p$  and  $\beta_\alpha$  represent the change in  $P_{ms}^b$  and  $\langle \alpha_s^b \rangle$  with increasing optical depth. Therefore, Equation 1 can be reformulated for each size class such that:

$$P_1^b = P_{ms1}^b [\exp(\beta_{p1}\tau)] \left[ 1 - \exp \left( - \frac{\langle \alpha_{s1}^b \rangle [\exp(\beta_{\alpha1}\tau)]}{P_{ms1}^b [\exp(\beta_{p1}\tau)]} \text{PAR} \right) \right] \quad (2)$$

$$P_2^b = P_{ms2}^b [\exp(\beta_{p2}\tau)] \left[ 1 - \exp \left( - \frac{\langle \alpha_{s2}^b \rangle [\exp(\beta_{\alpha2}\tau)]}{P_{ms2}^b [\exp(\beta_{p2}\tau)]} \text{PAR} \right) \right] \quad (3)$$

$$P^b = P_1^b F_1 + P_2^b F_2 \quad (4)$$

where, the subscripts 1 and 2 represent the combined pico-nanoplankton population and microplankton respectively. For each of the 15,013 individual primary production measurements PAR and  $\tau$  were provided.  $P^b$  was then computed by normalising each  $P$  measurement by [chl], then using [chl],  $F_1$  and  $F_2$  were computed using the Devred et al. (2006) model. Equations 2 to 4 were then fitted to the 15,013 measurements to derive  $P_{ms1}^b$ ,  $\langle \alpha_{s1}^b \rangle$ ,  $P_{ms2}^b$ ,  $\langle \alpha_{s2}^b \rangle$ ,  $\beta_{p1}$ ,  $\beta_{\alpha1}$ ,  $\beta_{p2}$  and  $\beta_{\alpha2}$  as shown in Table 1. The fitting

procedure used the same nonlinear least squares method as with the Devred et al. (2006) model.

Figure 3 shows the photosynthesis-irradiance curve plotted using the derived parameters for a variety of optical depths. Higher  $P_m^b$  values are found for combined nanoplankton than microplankton consistent with Bouman et al. (2005) and Kameda and Ishizaha (2005), but contradictory to Uitz et al. (2008) and Babin et al. (1996). Photophysiological parameters of microplankton display less variability with optical depth than combined nano-picoplankton, consistent with the knowledge that microplankton dominate in well mixed environments in comparison with combined nano-picoplankton, which generally prevail in more stratified environments.

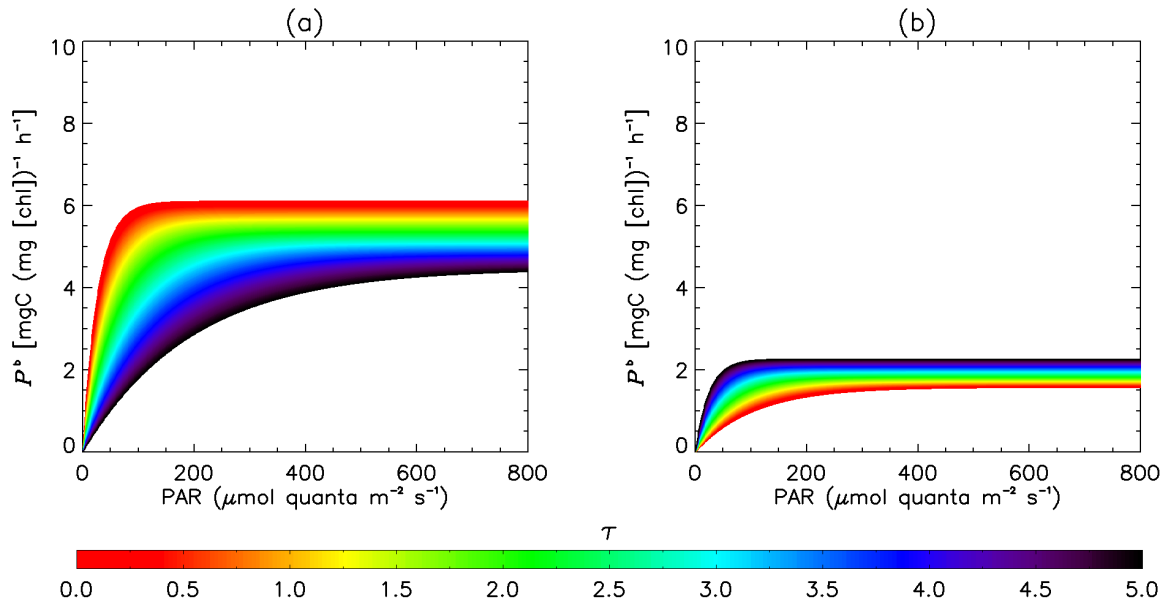


Figure 3. Photosynthesis-irradiance curve plotted using the derived parameters for a variety of optical depths ( $\tau$ ) for (a) combined nano-picoplankton and (b) microplankton.

Using the available-light model size-specific daily primary production within the euphotic zone (the depth of the water exposed to sufficient sunlight for photosynthesis), referred to as  $P_{eu}$  [ $\text{mg C m}^{-2} \text{ day}^{-1}$ ], can be calculated according to:

$$P_{eu1} = \int_{z=0}^{z_{eu}} \int_{t=\text{sunrise}}^{\text{sunset}} P_1^b(z, t)[\text{chl}_1](z) dz dt \quad (5)$$

$$P_{eu2} = \int_{z=0}^{z_{eu}} \int_{t=\text{sunrise}}^{\text{sunset}} P_2^b(z, t)[\text{chl}_2](z) dz dt \quad (6)$$

$$P_{eu} = P_{eu1} + P_{eu2} \quad (7)$$

where,  $z$  refers to the depth and  $t$  refers to the time. The  $P$  data was organised into vertical profiles. We rejected any profiles with less than six measurements in order to make an accurate calculation of  $P_{eu}$  for each profile, resulting in 1821 profiles. For each profile the day length, depth, and the euphotic depth were provided. Using equations 2 and 3 we calculated  $P_1^b$  and  $P_2^b$  for each measurement and we calculated  $[chl_1]$  and  $[chl_2]$  using the Devred et al. (2006) model and our derived parameters (Table 1). Then using equations 5 to 7, we predicted  $P_{eu}$  which is compared with the measured  $P_{eu}$  for each of the 1821 profiles in Figure 4. A strong correlation ( $r^2=0.7$ ) and low root mean square error percent (RMSE% = 54.0) is seen in Figure 4 indicating our model performs well when compared to the data to which it was parameterised.

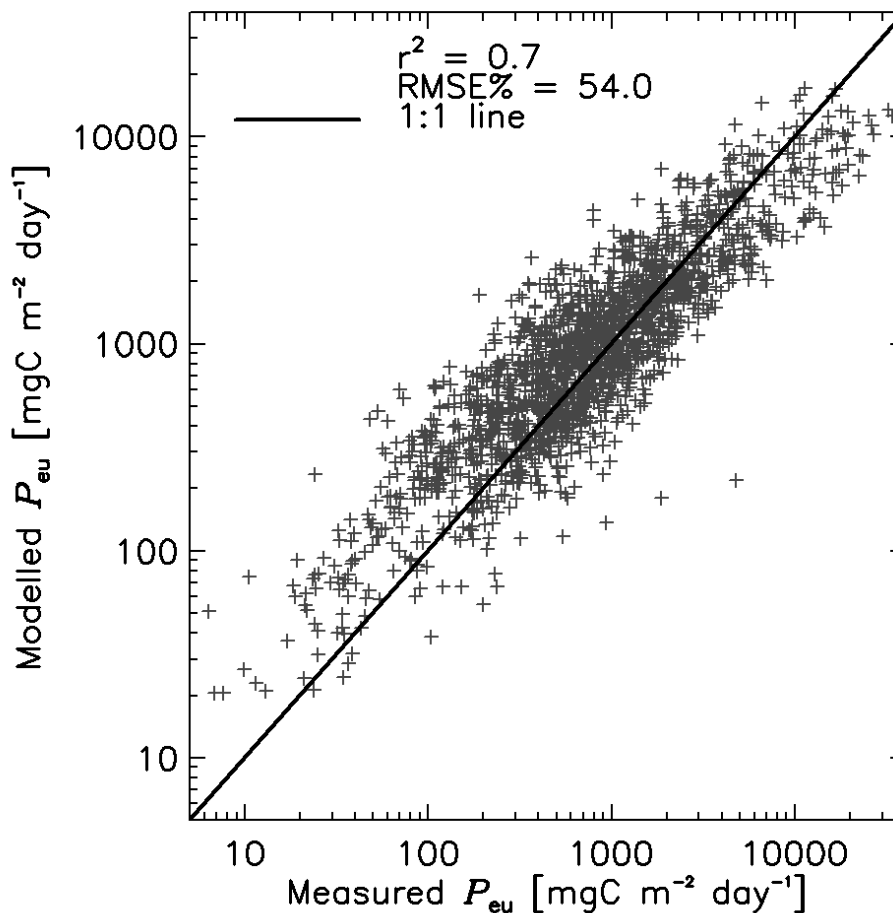


Figure 4. Measured  $P_{eu}$  against modelled  $P_{eu}$ .

In order to map size-specific  $P_{eu}$ , SeaWiFS Level 3 monthly binned composites of 2005 for diffuse attenuation coefficient ( $K_d$  490), the satellite derived chlorophyll-a concentration [ $chl_{sat}$ ] and PAR data, were downloaded from the NASA ocean colour website (<http://oceancolor.gsfc.nasa.gov>).  $Z_{eu}$  was then calculated from  $K_d(490)$  according to Behrenfeld and Falkowski (1997b) and we calculated  $K_{PAR}$  according to  $4.6 / Z_{eu}$ .

As the satellite chlorophyll-a concentration [ $chl_{sat}$ ] is only representative of the surface, we used the approach of Uitz et al. (2006) to predict the vertical chlorophyll-a profile from the surface chlorophyll-a concentration down to the euphotic depth, and by using the model of Devred et al. (2006), [ $chl_1$ ] and [ $chl_2$ ] were calculated at each depth. We modelled variations in PAR with depth down to  $Z_{eu}$  according to the Lambert-Beer law. We calculated the optical depth ( $\tau$ ) at each 10 metre interval by multiplying  $z$  by  $K_{PAR}$ . For each satellite pixel hourly  $P$ ,  $P_1$  and  $P_2$  were calculated at depth intervals of 10 metres down to  $Z_{eu}$ .  $P$ ,  $P_1$  and  $P_2$  were then integrated over the euphotic zone and day length of each pixel to derive  $P_{eu}$ ,  $P_{eu1}$  and  $P_{eu2}$  [ $\text{mg C m}^{-2} \text{ day}^{-1}$ ] for each month in 2005. Figure 5 shows the calculated  $P_{eu}$ ,  $P_{eu1}$  and  $P_{eu2}$  values for each month in 2005. On average, for 2005, we calculated total  $P_{eu}$  to be  $51.20 \pm 0.29 \text{ Gt C y}^{-1}$  of which, combined nano-picoplankton contributed to  $48.58 \pm 0.34 \text{ Gt C y}^{-1}$  (94.8%) and microplankton  $2.62 \pm 0.07 \text{ Gt C y}^{-1}$  (5.2%).

$P_{eu}$  derived for May 2005 is compared with that derived by Behrenfeld and Falkowski (1997b) (VGPM) and Joint and Groom (2000) for the same month in Figure 6. The VGPM is generally at the higher end of global  $P_{eu}$  estimates and the Joint and Groom (2000)  $P_{eu}$  model at the lower end (Barker, 2008). Therefore, the two models provide a good basis for comparison. For May 2005, we predict a  $P_{eu}$  value of  $3.627 \text{ Gt C mon}^{-1}$  which lies between the two estimates of  $2.686 \text{ Gt C mon}^{-1}$  for Joint and Groom (2000) and  $5.930 \text{ Gt C mon}^{-1}$  for the VGPM. Unlike the VGPM and the Joint and Groom (2000) model, our model predicts that of the  $3.627 \text{ Gt C mon}^{-1}$  calculated,  $3.384 \text{ Gt C mon}^{-1}$  (93.3%) was found to be attributed to combined nano-picoplankton and  $0.243 \text{ Gt C mon}^{-1}$  (6.7%) to microplankton.

## 4. Discussion

The geographical patterns of our model shown in Figure 6 are consistent with current knowledge about the biogeochemical provinces and ecological domains of the ocean (e.g. Hardman-Mountford et al., 2008; Longhurst, 1998). The eutrophic North Atlantic and areas of intense upwelling (e.g. Benguela and Canary upwelling zones) display higher  $P_{eu}$  values, and the subtropical gyres, often referred to as oligotrophic regions, display lower  $P_{eu}$  values.

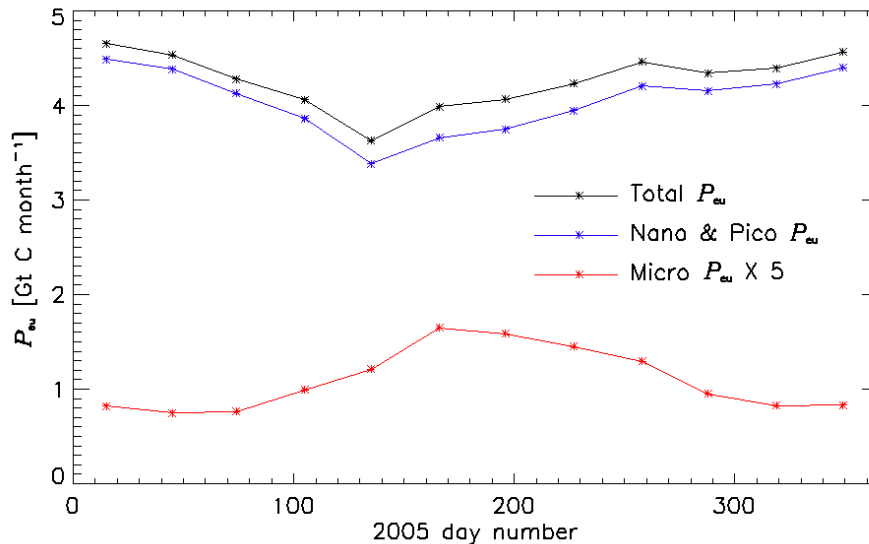


Figure 5. Timeseries of global primary production within the euphotic zone for the year 2005 calculated according to this study.

The main maps associated with this text indicate that microplankton contribute highly to global  $P_{eu}$  in coastal regions, as well as in areas of upwelling, the sub-arctic in May, and the sub-antarctic in November. Their contribution is shown to reduce in equatorial regions and is virtually non-existent in the oligotrophic regions. The combined nanoplankton  $P_{eu}$  contribution is more stable globally with slightly higher  $P_{eu}$  contributions in mid-high latitudes. In comparison to May 2005, for November 2005, we calculated a total  $P_{eu}$  value of 4.391 Gt C mon $^{-1}$ , of this, combined nano-picoplankton contribute to 4.226 Gt C mon $^{-1}$  (96.2%) and microplankton 0.165 Gt C mon $^{-1}$  (3.8%). Results support estimates by [Hirata et al. \(2009\)](#) which indicate combined nano- picoplankton contribute more to  $P$  due to a larger spatial coverage. [Carr et al. \(2006\)](#) conducted a comparison of 24 satellite  $P$  models and found global estimates for total  $P$  varied from 30 to 70 Gt C y $^{-1}$  depending on the model used. In the [Carr et al. \(2006\)](#) study, a mean value of 50.7 Gt C y $^{-1}$  was found when comparing all the 24 satellite models. This value compliments our estimate of  $51.20 \pm 0.29$  Gt C y $^{-1}$  for 2005.

## 5. Conclusion

The primary maps associated with this text combine two established satellite models, one that estimates size-specific phytoplankton biomass and another that calculates primary production, and they provide an estimation of size-specific primary production on a global scale. The [Devred et al. \(2006\)](#) model was fitted to a large pigment dataset

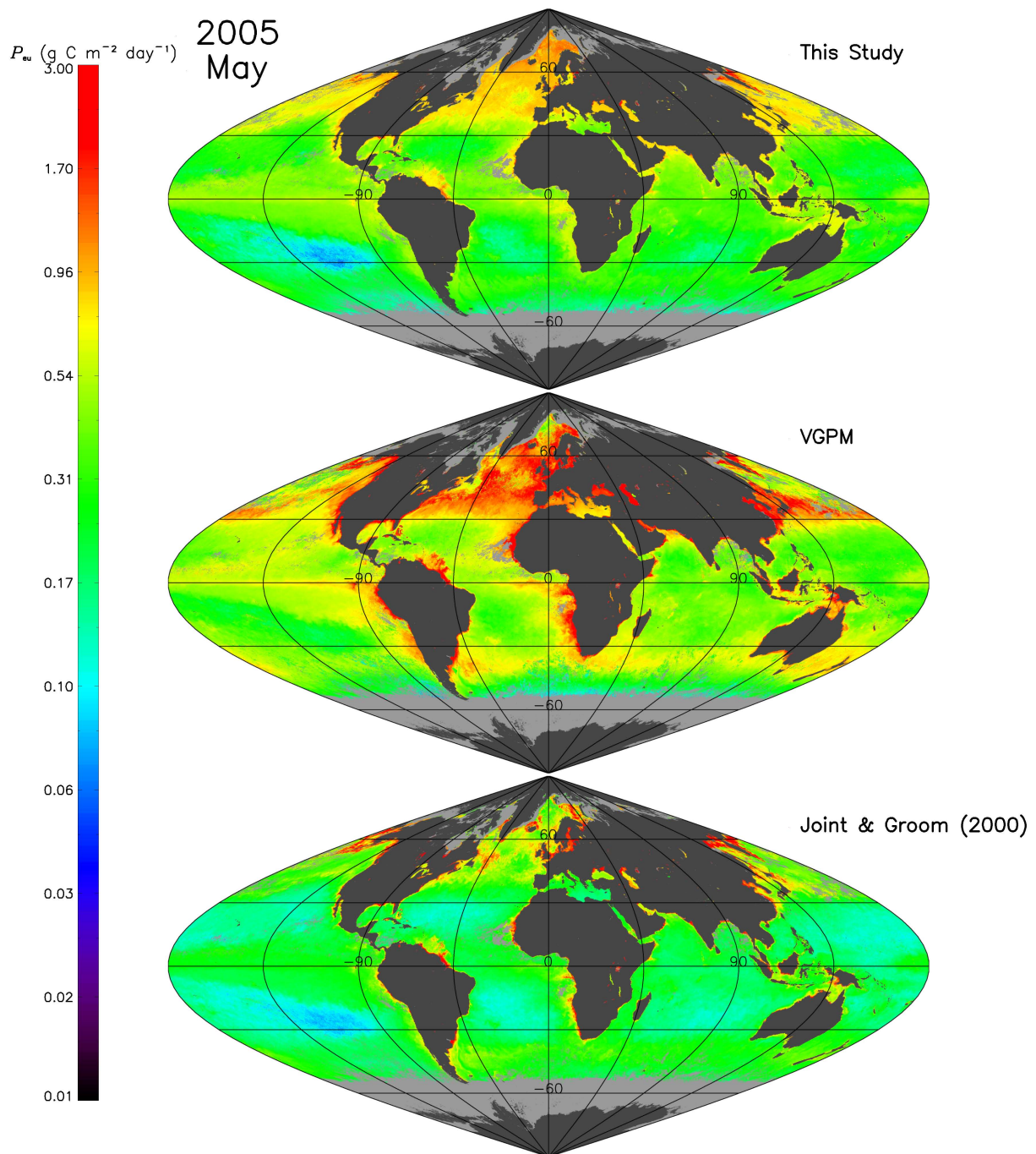


Figure 6. Global primary production for May 2005 calculated according to this study (top), the vertically generalised production model (Behrenfeld and Falkowski, 1997b, VGPM) (middle), and Joint and Groom (2000) (bottom).

from the global ocean, before being integrated into an available-light primary production model.

Maps of May and November 2005 (primary maps affiliated with this text) were produced which highlight that combined nano- and picoplankton contribution to  $P_{eu}$  is relatively stable regionally whereas, microplankton vary strongly between regions. Global estimates of  $P_{eu}$  are consistent with previous models with the added advantage over previous techniques of deriving size-specific  $P_{eu}$  rates.

Following the approach of Jennings et al. (2008), such size-specific  $P_{eu}$  maps can be used to improve metabolic scaling models used to predict the potential biomass, production, size, and trophic structure of consumer communities from satellite data. This is particularly beneficial in environments that are difficult to sample directly. Furthermore, such a model could be used in operational and sustainable fisheries management. Size-specific  $P_{eu}$  maps can also be used to validate and improve multi-phytoplankton ecosystem models (Anderson, 2005) (e.g. Diat-HadOCC at the UK Met Office), with an added advantage over *in situ* measurements of providing a synoptic viewpoint. This will ultimately enhance our understanding of the interaction between phytoplankton and our environment, which is needed to help set baselines for human and climate impacts on global scales.

## Software

Data processing was conducted using IDL Version 6.3 computer coding language. Data was downloaded freely from the NASA ocean color website (<http://oceancolor.gsfc.nasa.gov>) and is in accordance with the SeaWiFS Research Data Use Terms and Agreements.

## Acknowledgements

The NASA SeaWiFS project team is acknowledged for satellite data and all contributors to the NOMAD data set for *in situ* pigment data. Thanks to the officers and crew of RRS James Clark Ross and RRS Discovery and all scientists who helped in the acquisition and analyses of AMT data. Thanks also to interesting conversations with Dr Shubha Sathyendranath and Dr Trevor Platt. This work is funded by the Natural Environment Research Council, UK, through a PhD studentship to the National Centre for Earth Observation. We also thank the two reviewers for useful comments.

## References

- AIKEN, J., PRADHAN, Y., BARLOW, R., LAVENDER, S., POULTON, A., HOLLIGAN, P. and HARDMAN-MOUNTFORD, N. J. (2009) Phytoplankton pigments and functional types in the Atlantic Ocean: a decadal assessment, 1995-2005, *Deep-Sea Research II*, 56, 899–917, doi:10.1016/j.dsr2.2008.09.017.
- ANDERSON, T. R. (2005) Plankton functional type modelling: running before we can walk?, *Journal of Plankton Research*, 27, 1073–1081.
- BABIN, M., MOREL, A., CLAUSTRE, H., BRICAUD, A., KOLBER, Z. S. and FALKOWSKI, P. G. (1996) Nitrogen- and irradiance-dependant variations of the maximum quantum yield of carbon fixation in eutrophic, mesotrophic and oligotrophic marine systems, *Deep-Sea Research I*, 43, 1241–1272.
- BARKER, K. (2008) A Novel Technique to Estimate Primary Production Directly From Earth Observation Data: An Inherent Optical Property Approach, Unpublished PhD thesis, School of Earth, Ocean and Environmental Sciences, University of Plymouth.
- BEHRENFELD, M. J. and FALKOWSKI, P. G. (1997a) A consumer's guide to phytoplankton primary productivity models, *Limnology and Oceanography*, 42, 1479–1491.
- BEHRENFELD, M. J. and FALKOWSKI, P. G. (1997b) Photosynthetic Rates Derived from Satellite-Based Chlorophyll Concentration, *Limnology and Oceanography*, 42 (1), 1–20.
- BOUMAN, H., PLATT, T., SATHYENDRANATH, S. and V, S. (2005) Dependence of light-saturated photosynthesis on temperature and community structure, *Deep Sea Research*, 52, 1284–1299.
- CARR, M. E., FRIEDRICHS, M. A. M., SCHMELTZ, M., AITA, M. N., ANTOINE, D., ARRIGO, K. R., ASANUMA, I., AUMONT, O., BARBER, R., BEHRENFELD, M., BIDIGARE, R., BUITENHUIS, E. T., CAMPBELL, J., CIOTTI, A., DIERSSEN, H., DOWELL, M., DUNNE, J., ESAIAS, W., GENTILI, B., GREGG, W., GROOM, S., HOEPPFNER, N., ISHIZAKA, J., KAMEDA, T., QUERE, C. L., LOHRENZ, S., MARRA, J., MELIN, F., MOORE, K., MOREL, A., REDDY, T. E., RYAN, J., SCARDI, M., SMYTH, T., TURPIE, K., TILSTONE, G., WATERS, K. and YAMANAKA, Y. (2006) A comparison of global estimates of marine primary production from ocean color, *Deep-Sea Research II*, 53, 741–770.
- CHISHOLM, S. W. (1992) Phytoplankton Size, In FALKOWSKI, P. and WOODHEAD, A., (eds.) *Primary Productivity and Biogeochemical Cycles in the Sea*, Springer, New York., pp. 213–237.
- CIOTTI, A. M. and BRICAUD, A. (2006) Retrievals of a size parameter for phytoplankton and spectral light absorption by coloured detrital matter from water-leaving radiances at SeaWiFS channels in a continental shelf off Brazil, *Limnology and Oceanography: Methods*, 4, 237–253.
- DEVRED, E., SATHYENDRANATH, S., V, S., MAAS, H., ULLOA, O. and PLATT, T. (2006) A two-component model of phytoplankton absorption in the open ocean: Theory and applications, *Journal of Geophysical Research*, 111, C03,011, doi:10.1029/2005JC002,880.
- FALKOWSKI, P. G., KATZ, M. E., KNOLL, A. H., QUIGG, A., RAVEN, J. A., SCHOFIELD, O. and TAYLOR, F. J. R. (2004) The evolution of modern eukaryotic phytoplankton, *Science*, 305, 354–360.
- FIELD, C. B., BEHRENFELD, M. J., RANDERSON, J. T. and FALKOWSKI, P. (1998) Primary production of the biosphere: integrating terrestrial and oceanic components, *Science*, 281, 237–240.

- HARDMAN-MOUNTFORD, N. J., HIRATA, T., RICHARDSON, K. A. and AIKEN, J. (2008) An objective methodology for the classification of ecological pattern into biomes and provinces for the pelagic ocean, *Remote Sensing of Environment*, 112, 3341–3352.
- HIRATA, T., AIKEN, J., HARDMAN-MOUNTFORD, N. J., SMYTH, T. J. and BARLOW, R. G. (2008) An absorption model to derive phytoplankton size classes from satellite ocean colour, *Remote Sensing of Environment*, 112, 3153–3159.
- HIRATA, T., HARDMAN-MOUNTFORD, N. J., BARLOW, R., LAMONT, T., BREWIN, R. J. W., SMYTH, T. and AIKEN, J. (2009) An inherent optical property approach to the estimation of size-specific photosynthetic rates in eastern boundary upwelling zones from satellite ocean colour: an initial assessment, *Progress in Oceanography*, 83, 393–397.
- HOUSE, J. I., PRENTICE, I. C. and LE QUÉRÉ, C. (2002) Maximum impacts of future reforestation or deforestation on atmospheric CO<sub>2</sub>, *Global Change Biology*, 8, 1047–1052.
- JENNINGS, S., MÉLIN, F., BLANCHARD, J. L., FORSTER, R. M., DULVY, N. K. and WILSON, R. W. (2008) Global-scale predictions of community and ecosystem properties from simple ecological theory, *Proceedings of the Royal Society B*, 275, 1375–1383 doi:10.1098/rspb.2008.0192.
- JOINT, I. and GROOM, S. B. (2000) Estimation of Phytoplankton Production from Space: Current Status and Future Potential of Satellite Remote Sensing, *Journal of Experimental Marine Biology and Ecology*, 250, 233–55.
- KAMEDA, T. and ISHIZAHA, J. (2005) Size-fractionated Primary Production Estimated by a two-phytoplankton community model applicable to ocean color remote sensing, *Journal of Oceanography*, 61, 663–672.
- LE QUÉRÉ, C., HARRISON, S. P., PRENTICE, C. I., BUITENHUIS, E. T., AUMONT, O., BOPP, L., CLAUSTRE, H., CUNHA, L. C. D., GEIDER, R., GIRAUD, X., KLAAS, C., KOHFELD, K. E., LEGENDRE, L., MANIZZA, M., PLATT, T., RIVKIN, R., SATHYENDRANATH, S., UITZ, J., WATSON, A. J. and WOLF-GLADROW, D. (2005) Ecosystem dynamics based on plankton functional types for global ocean biogeochemistry models, *Global Change Biology*, 11, 2016–2040.
- LONGHURST, A., SATHYENDRANATH, S., PLATT, T. and CAVERHILL, C. (1995) An estimate of global primary production in the ocean from satellite radiometer data, *Journal of Plankton Research*, 17.
- LONGHURST, A. R. (1998) *Ecological Geography of the Sea*, Academic Press, San Diego, 398 pp.
- MOREL, A. (1991) Light and Marine Photosynthesis: A Spectral Model with Geochemical and Climatological Implications, *Progress in Oceanography*, 26, 263–306.
- NAIR, A., SATHYENDRANATH, S., PLATT, T., MORALES, J., V, S., FORGET, M.-H., DEVRED, E. and BOUMAN, H. (2008) Remote sensing of phytoplankton functional types, *Remote Sensing of Environment*, 112, 8, 3366–3375.
- PLATT, T., GALLEGOS, C. L. and HARRISON, W. G. (1980) Photoinhibition of photosynthesis in natural assemblage of marine phytoplankton, *Journal of Marine Research*, 38, 687–701.
- PLATT, T. and SATHYENDRANATH, S. (1988) Oceanic Primary Production: Estimation by Remote Sensing at Local and Regional Scales, *Science*, 241, 1613–1620.

- PRESS, W. H., KEUKOLSKY, S. A., VETTERING, W. T. and FLANNERY, B. P. (1992) Levenberg-Marquard Method, In *Numerical Recipes in C: The Art of Scientific computation*, Cambridge University Press, New York, pp. 542–547.
- SATHYENDRANATH, S., LONGHURST, A. R., CAVERHILL, C. M. and PLATT, T. (1995) Regionally and seasonally differentiated primary production in the North Atlantic, *Deep-Sea Research I*, 42, 1773–1802.
- SATHYENDRANATH, S. and PLATT, T. (2007) Spectral effects in bio-optical control on the ocean system, *Oceanologia*, 49, 5–39.
- SATHYENDRANATH, S., V, S., COTA, G., MAAS, H. and PLATT, T. (2001) Remote sensing of phytoplankton pigments: a comparison of empirical and theoretical approaches, *International Journal of Remote Sensing*, 22, 249–273.
- SIEBURTH, J. M., V, S. and LENZ, J. (1978) Pelagic ecosystem structure: Heterotrophic compartments of the plankton and their relationship of plankton size fractions, *Limnology and Oceanography*, 23, 1256–1263.
- STEEMAN-NIELSEN, E. (1952) The Use of Radio-Active Carbon ( $C^{14}$ ) for Measuring Organic Production in the sea, *Journal du Conseil International de l'Exploration de la Mer*, 18, 117–140.
- UITZ, J., CLAUSTRE, H., MOREL, A. and HOOKER, S. B. (2006) Vertical distribution of phytoplankton communities in open ocean: An assessment based on surface chlorophyll, *Journal of Geophysical Research*, 111, CO8005, doi:10.1029/2005JC003,207.
- UITZ, J., HUOT, Y., BRUYANT, F., BABIN, M. and CLAUSTRE, H. (2008) Relating phytoplankton photophysiological properties to community structure on large scales, *Limnology and Oceanography*, 52, 614–630.
- VIDUSSI, F., CLAUSTRE, H., MANCA, B. B., LUCHETTA, A. and MARTY, J. C. (2001) Phytoplankton pigment distribution in relation to upper thermocline circulation in the eastern Mediterranean Sea during winter, *Journal of Geophysical Research*, 106(C9), 19,939–19,956.
- WERDELL, P. J. and BAILEY, S. W. (2005) An improved in situ bio-optical data set for ocean colour algorithm development and satellite data production validation, *Remote Sensing Environment*, 98, 122–140.